Supplemental Material for

Effect of sticker clustering on the dynamics of associative networks

Irina Mahmad Rasid,[†] Changwoo Do, Niels Holten-Andersen[*,†] and Bradley D. Olsen*[*,‡]*

[†] Department of Materials Science and Engineering, Massachusetts Institute of Technology, 77 Massachusetts Avenue, Cambridge, Massachusetts 02139, United States

Neutron Scattering Division, Oak Ridge National Laboratory, Oak Ridge, Tennessee 37830, United States

[‡] Department of Chemical Engineering, Massachusetts Institute of Technology, 77 Massachusetts Avenue, Cambridge, Massachusetts 02139, United States

*Correspondence should be addressed to B.D.O (bdolsen@mit.edu) and N.H.A (holten@mit.edu)

Table of Contents

A. Supplementary Figures cited in the Main Text

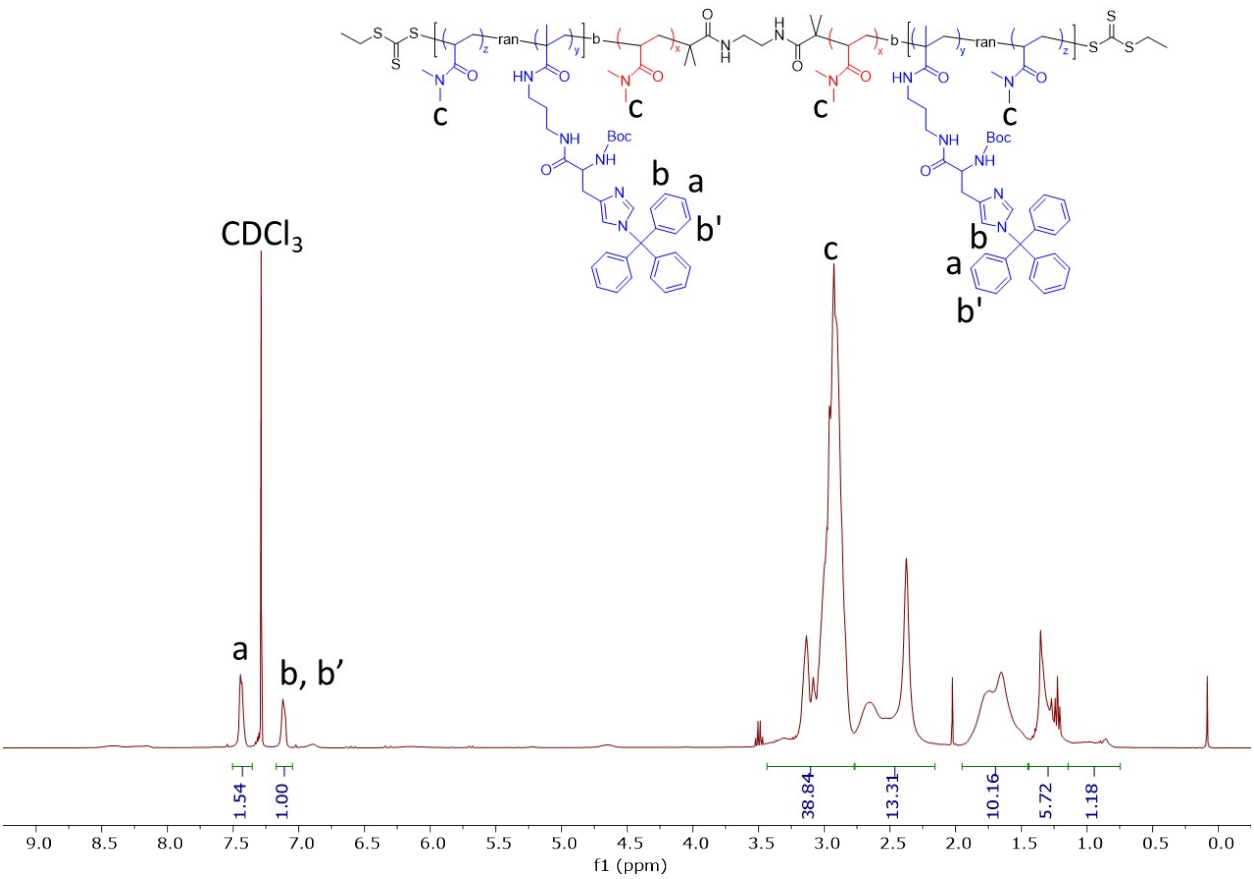

Figure S1. ^{1}H NMR characterization of the PDMA polymer with protected histidine side groups clustered at the chain ends ($CDCl_3$, 400 MHz). Peaks assigned in the spectrum are used for calculating the monomer ratio in the polymers. For the peak labelled c, the integration is from δ = 2.75 – 3.20 ppm.

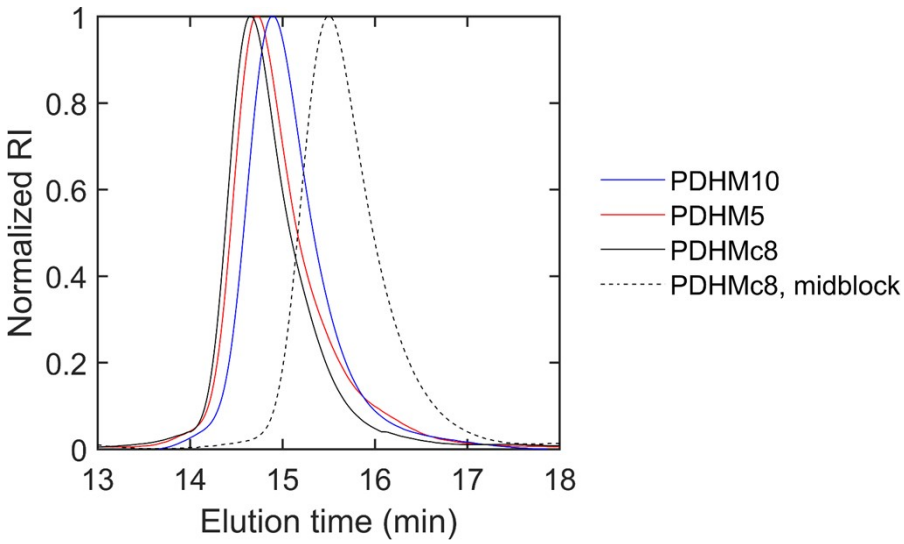

Figure S2. The polymers were characterized using DMF GPC prior to deprotection. All samples were prepared at 10 mg/mL in DMF with 0.02 M LiBr. The weight-average molar mass, M_w, dispersity, $Đ$ and dn/dc used for each polymer are: PDHM10 - M_w = 30.7 kg mol^{-1}, $Đ$ = 1.04, dn/dc = 0.083. PDHM5 - M_w = 26.6 kg mol^{-1}, $Đ$ = 1.03, dn/dc = 0.085. PDHMc8 - M_w = 29.5 kg mol^{-1}, $Đ$ = 1.03, dn/dc = 0.087. PDHMc8, midblock - M_w = 15.9 kg mol^{-1}, $Đ$ = 1.06, dn/dc = 0.087. The dn/dc values used for each polymer was measured using a Wyatt Optilab T-rEX differential refractive index detector.

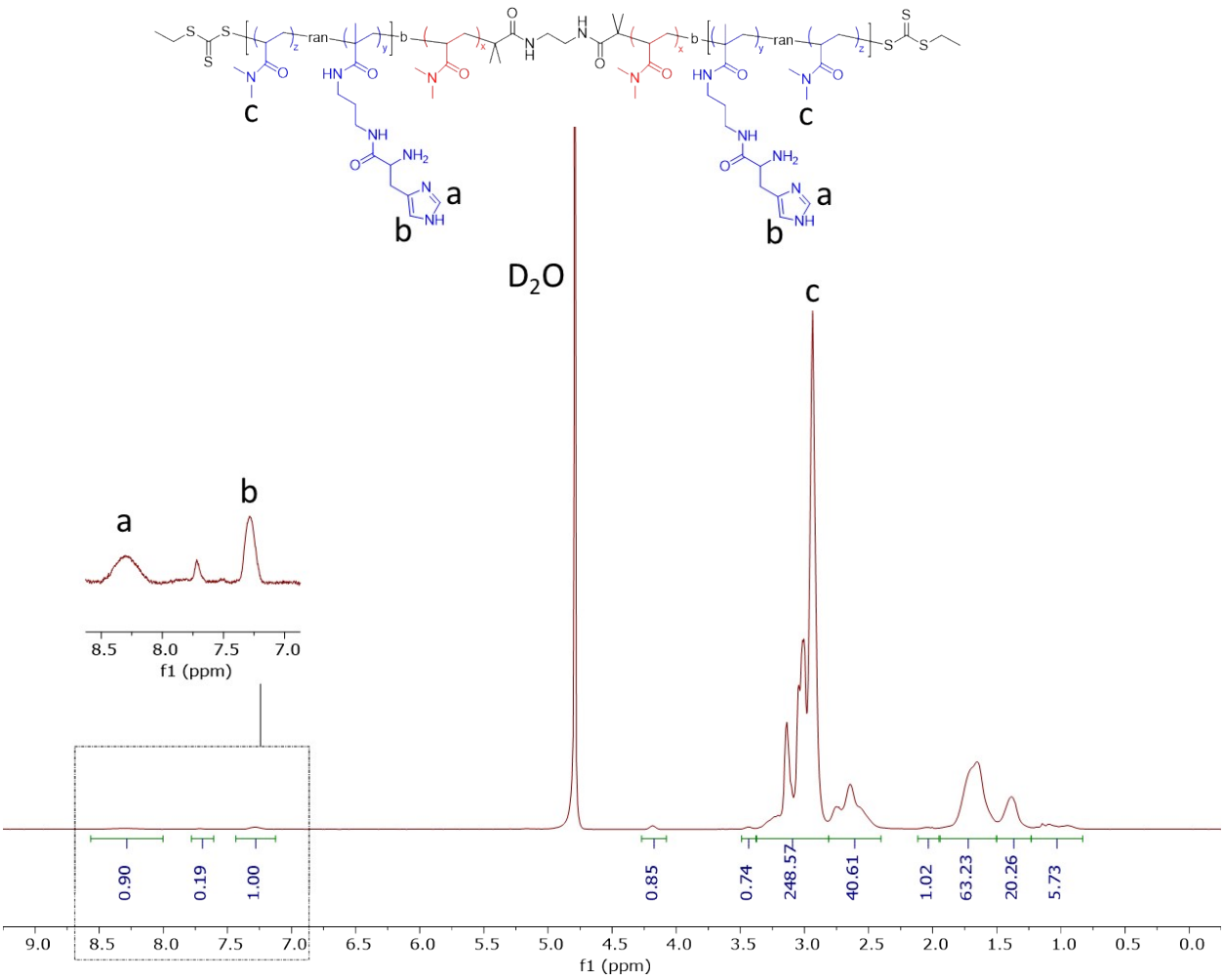

Figure S3. ^{1}H NMR characterization of the PDMA polymer with histidine side groups clustered at the chain ends, after deprotection (D_2O, 400 MHz). The positions of peaks a and b are slightly different depending on the residual TFA remaining in the polymer.

B. Supplementary Tables cited in the Main Text

The results of the fits to a correlation length model for the SANS data reported in Figure 4 are shown in Table S1. The scattering intensity in the model is given by

$$I(q) = \frac{A}{q^n} + \frac{C}{1 + (q\xi)^m} + B \quad (1)$$

where $I(q)$ is the scattering intensity, q is the scattering vector, n is the Porod exponent, ξ is the Lorentzian screening length, m is the Lorentzian exponent and B is the incoherent scattering contribution. A and C are the Porod and Lorentzian scale, respectively.

Table S1. Results of the fits to the correlation length model and aggregate size estimate from the crossover of the power law fits.

	PDHMc8	PDHM5	PDHM10
A	$(1.4 \pm 0.1) \times 10^{-5}$	$(2.7 \pm 0.1) \times 10^{-4}$	$(4.4 \pm 0.1) \times 10^{-6}$
n	3.032 ± 0.008	2.33 ± 0.01	3.17 ± 0.02
C	9.96 ± 0.01	10.03 ± 0.01	20.03 ± 0.01
m	2.019 ± 0.005	2.129 ± 0.006	1.943 ± 0.005
ξ (Å)	6.181 ± 0.008	5.902 ± 0.008	7.24 ± 0.01
B (cm^{-1})	0.1001 ± 0.0003	0.1266 ± 0.0003	0.1543 ± 0.0003
Clustering strength (cm^{-1})	260 ± 30	104 ± 9	180 ± 20

C. Note on the use of TFA for deprotection and pH of the gels

While TFA is a common choice for deprotection chemistry, it is difficult to completely remove TFA from the product following the reaction. For the gels used in this study, the residual TFA alters the pH of the gels, and the properties of the histidine-nickel coordination complex have been shown to strongly depend on its pH.[1] To avoid issues with reproducibility of the gel properties, the polymers are dissolved in Milli-Q water and spun down using centrifugal filters with MWCO of 3 kDa. This process is repeated four times and is successful at removing most of the residual TFA, as evidenced by the shift in the position of peaks a and b in Figure S3.

Following the filtration step, the volume of 1 M NaOH in 100 mM bis-tris required to adjust the pH of the solution to seven was determined by titration with dilute solution. The polymers were dissolved in a solution of 0.1 M KCl, with a concentration of approximately 15 mg in 1 mL. The pH was recorded with a pH probe while aliquots of 0.1 M KOH was titrated into the solution (Figure S4). The volume of 0.1 M KOH needed to arrive at pH 7 is used to calculate the volume of 1 M NaOH stock solution added for each polymer.

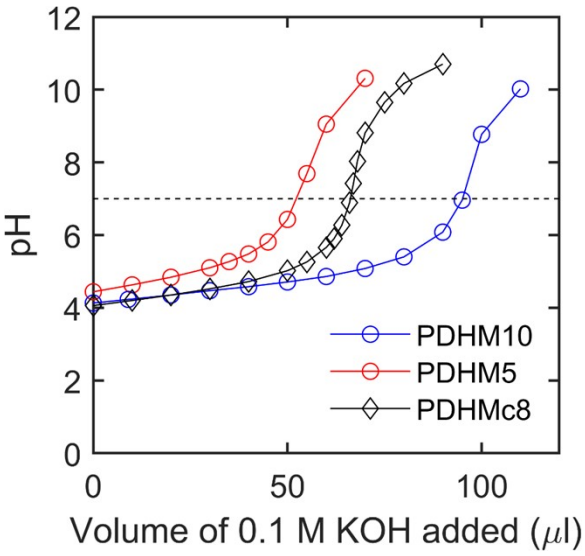

Figure S4. After deprotection and removal of residual TFA by filtration with water, ~15 mg of the polymers [PDHM5 (15.1 mg), PDHMc8 (16.8 mg) and PDHM10 (15.1 mg)] were dissolved in 1 mL of 0.1 M KCl. To each solution, the appropriate amount of Ni^{2+} was added such that the ratio of His:Ni^{2+} was 2:1. The pH values were then recorded as aliquots of 0.1 M KOH was added.

D. Calculation of concentration regimes

From reptation theory, the entanglement concentration is

$$\phi_e = \left(\frac{N_{e,0}}{N}\right)^{3\upsilon - 1} \tag{2}$$

where $N_{e,0}$ is the number of monomers between entanglements in a melt, N is the degree of polymerization of the polymer, and υ is the Flory exponent. Since $N_{e,0}$ of PDMA has not been reported in the literature to the author's knowledge, the entanglement concentration for the histidine modified PDMA polymers in this study is estimated by comparison to literature data.

The entanglement concentration of PDMA at a molecular weight of 3.4×10^3 kg mol^{-1} is 0.81% (w/w), determined from the transition of zero-shear-rate viscosity of PDMA aqueous solution.[2] From eq 2, it can be shown that:

$$\phi_{e,2} = \left(\frac{N_1}{N_2}\right)^{3\upsilon - 1}\phi_{e,1} \tag{3}$$

where the subscripts 1 and 2 denote the case from the literature and from the current study, respectively. Therefore, the entanglement concentration for the polymers synthesized in this study was calculate using eq. 2, with $\upsilon = 0.588$ under the assumption of good solvent conditions.

Similarly, the chain overlap concentration can be estimated as

$$\phi_{overlap,2} = \left(\frac{N_1}{N_2}\right)^{3\upsilon - 1}\phi_{overlap,1} \tag{4}$$

which uses the overlap concentration of PDMA at a molecular weight of 3.4×10^3 kg mol^{-1} of

0.07% (w/w). [2]

The strand (between stickers) overlap concentration[3] can be estimated as

$$\phi_s \approx l^{1-3\upsilon} \tag{5}$$

where l is the spacing between stickers.

E. Construction of master curves from time-temperature superposition

The master curves in Figure 2 were constructed by calculating the vertical, b_T and horizontal, a_T shift factors for each gel. The vertical shift factors were experimentally determined using the values of the loss modulus, G" at the low frequency maxima such that

$$b_T = \frac{G''_{Maxima,T_0}}{G''_{Maxima,T}} \tag{6}$$

where T_0 = 35 °C was used as the reference temperature. The normalized G' and G" were then horizontally shifted to construct the master curves. The horizontal shift factors show good agreement with the Arrhenius model, consistent with the experimental temperature being well above the glass transition temperature (Figure S5).

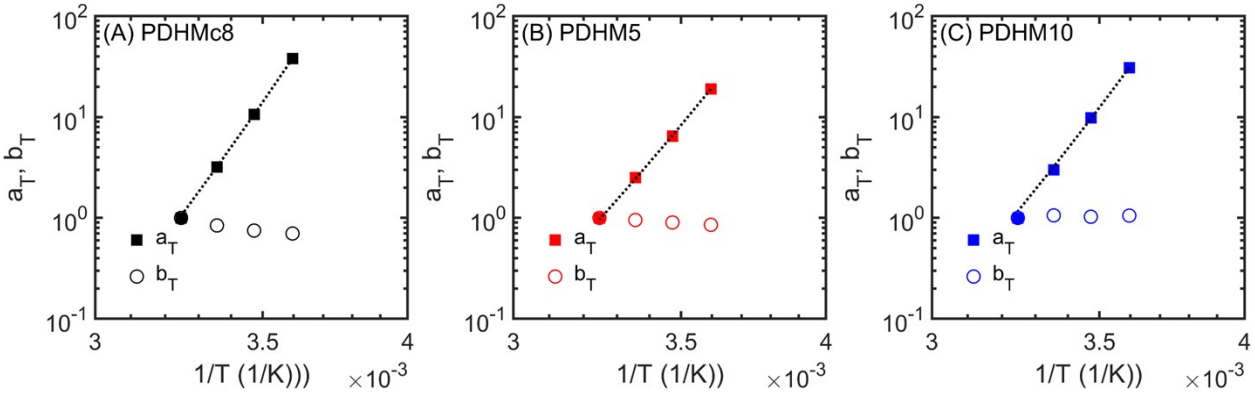

Figure S5. The vertical, b_T and horizontal, a_T shift factors for each gel. Dashed lines with a_T are fits to the empirical Arrhenius model.

F. Additional data for gels prepared at 30% (w/v)

The data collected for PDHMc8 and PDHM5 gels prepared at 30% (w/v) showed the same trends as the gels at 25% (w/v). Note that higher concentrations were not investigated as this would be above the entanglement concentration, and the time scales of the PDHM10 gel at 30% (w/v) were not experimentally accessible. The similarity between the two concentrations was seen in the fact that the plateau modulus shows $G_{p,c8} < G_{p,5}$ and the relaxation time shows $\tau_{c8} > \tau_5$ (Figure S6 and Figure S7). The activation energy as calculated from an empirical Arrhenius fit to the plot of τ vs $1/T$ (Figure S7), E_{app} was found to be $E_{app,c8}$ = 81 ± 2 kJ mol^{-1} and $E_{app,5}$ = 69 ± 2 kJ mol^{-1}.

The diffusion data collected at 35 °C for the PDHMc8 and PDHM5 gels at 30% (w/v) also showed $\langle\tau_{c8}\rangle < \langle\tau_5\rangle$ for the entire range of d^2 that was measured (Figure S8).

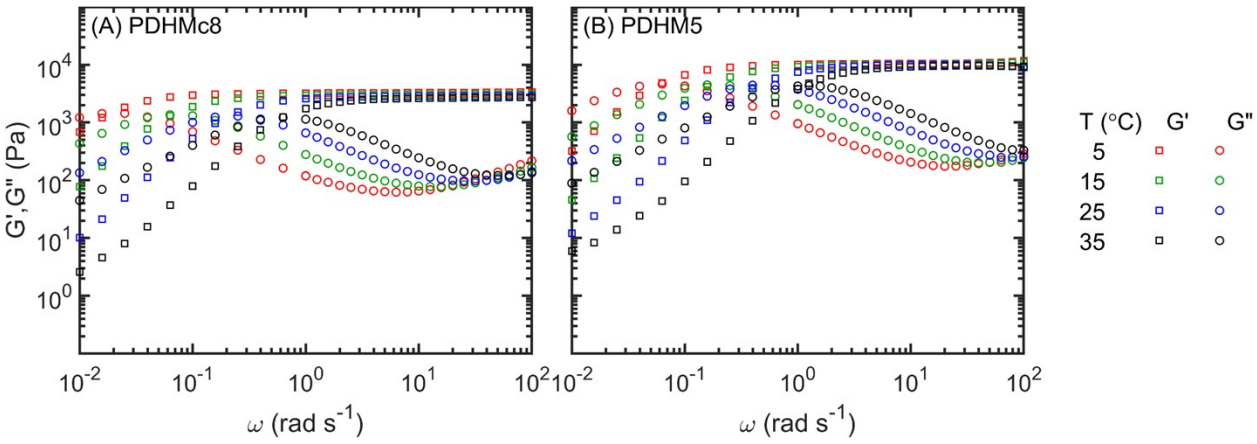

Figure S6. Frequency sweeps for (A) PDHMc8 and (B) PDHM5 at 30% (w/v), measured at 5, 15, 25 and 35 °C.

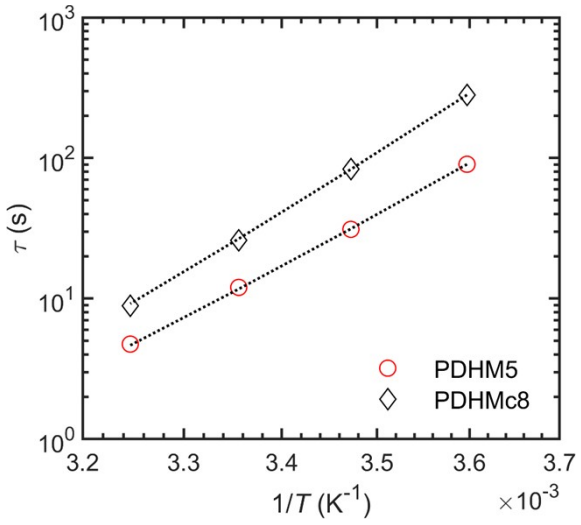

Figure S7. Network relaxation time τ at varying temperatures for gels at 30% (w/v). The black dashed lines are fits to an Arrhenius law.

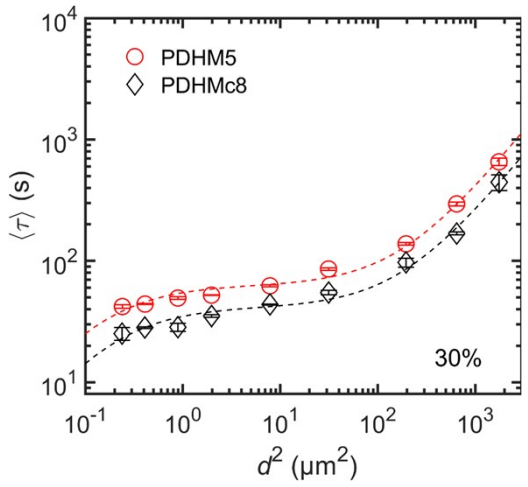

Figure S8. Plot of $\langle\tau\rangle$ vs d^2 for PDHM5 and PDHMc8, measured at 35 °C. Both gels were prepared at a concentration of 30% (w/v). The dashed lines are fits to the two-state model. Error bars represent one standard deviation of measurements performed in triplicate.

G. Additional NMR Spectra

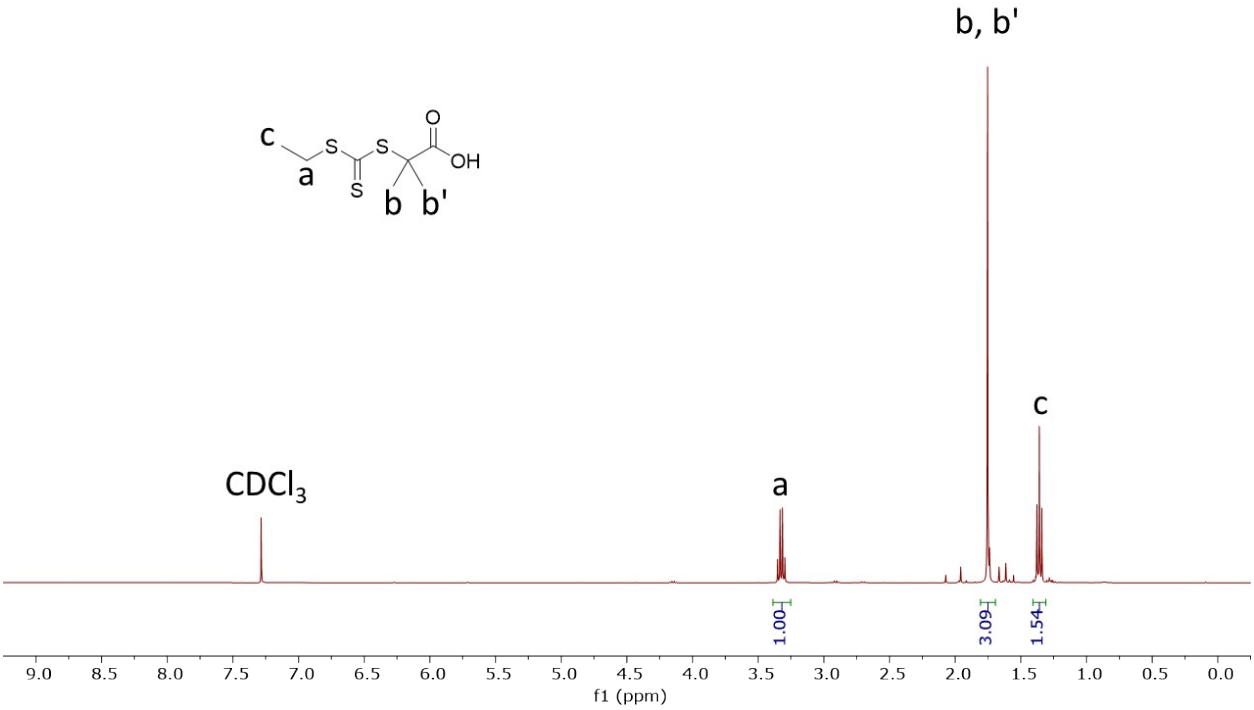

Figure S9. ^{1}H NMR characterization of 2-(((ethylthio)carbonothioyl)thio)-2-methylpropanoic acid ($CDCl_3$, 400 MHz).

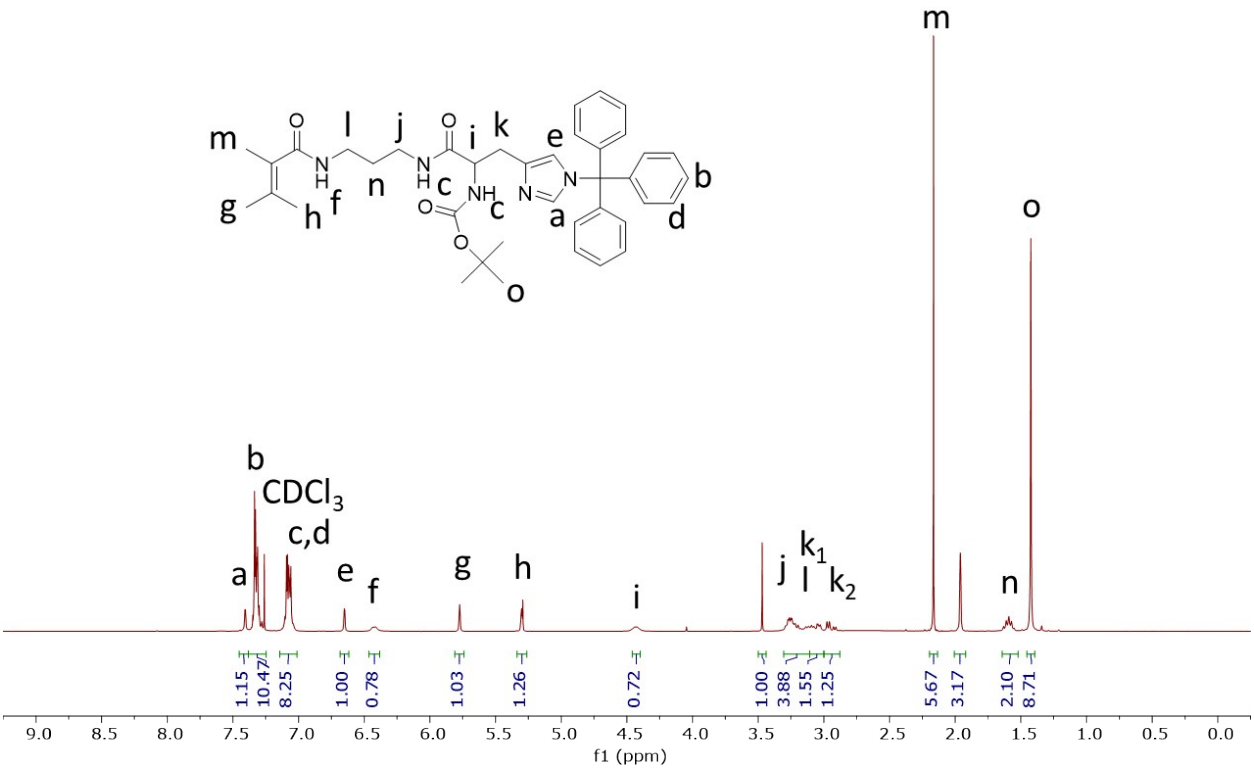

Figure S10. ^{1}H NMR characterization of Boc-Nim-trityl-N-3-methacrylamidopropyl-L-Histidinamide ($CDCl_3$, 400 MHz).

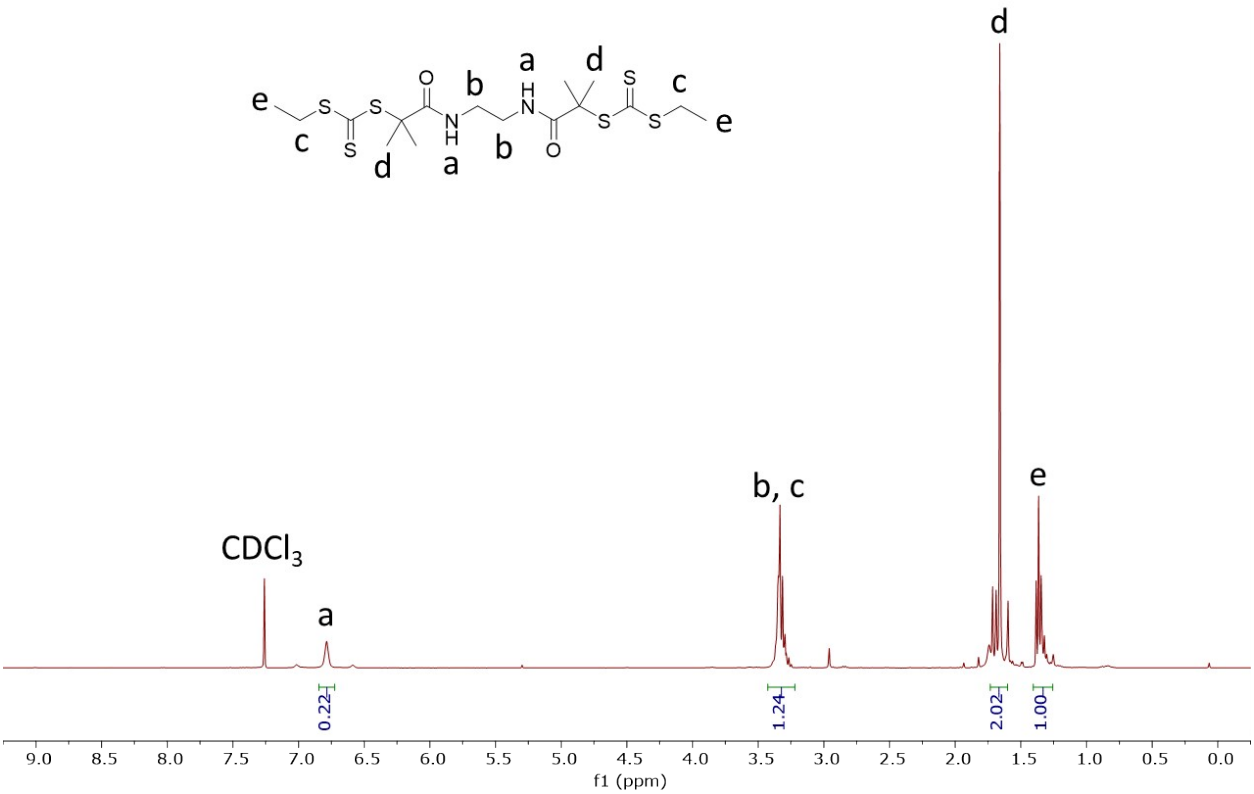

Figure S11. ^{1}H NMR characterization of the EMP dimer ($CDCl_3$, 400 MHz).

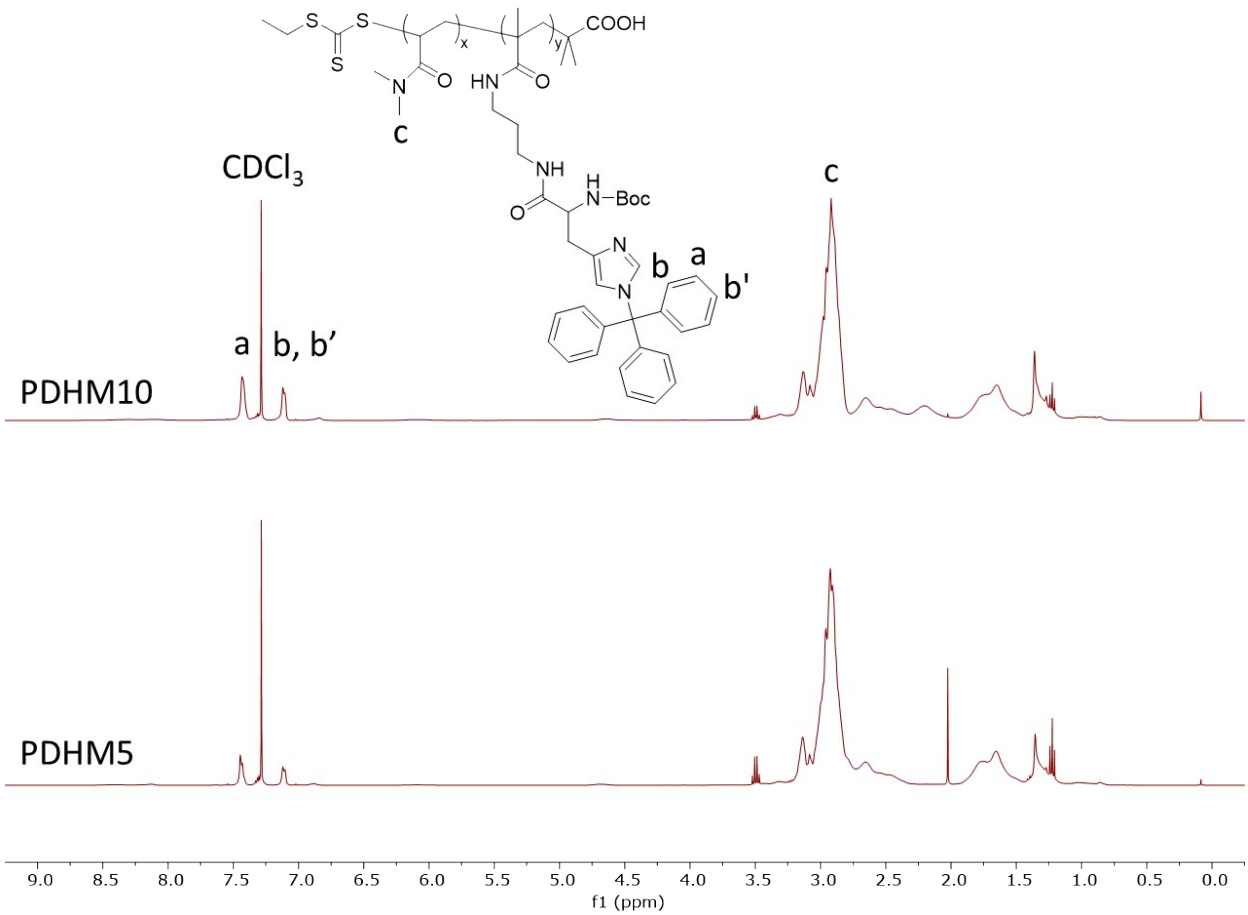

Figure S12. ^{1}H NMR characterization of the random PDMA copolymers with protected histidine side groups ($CDCl_3$, 400 MHz). Peaks assigned in the spectrum are used for calculating the monomer ratio in the polymers. For peak labelled c, the integration is from δ = 2.75 – 3.20 ppm.

H. References

1. Fullenkamp, D. E.; He, L.; Barrett, D. G.; Burghardt, W. R.; Messersmith, P. B., Mussel-inspired histidine-based transient network metal coordination hydrogels. *Macromolecules* **2013,** *46* (3), 1167-1174.
2. Fredlake, C. P.; Hert, D. G.; Kan, C. W.; Chiesl, T. N.; Root, B. E.; Forster, R. E.; Barron, A. E., Ultrafast DNA sequencing on a microchip by a hybrid separation mechanism that gives 600 bases in 6.5 minutes. *Proc Natl Acad Sci U S A* **2008,** *105* (2), 476-81.
3. Rubinstein, M.; Semenov, A. N., Dynamics of entangled solutions of associating polymers. *Macromolecules* **2001,** *34* (4), 1058-1068.